American Mineralogist, Volume 70, pages 1232–1237, 1985

Oriented hematite inclusions in sillimanite

MICHAEL E. FLEET AND MAKOTO ARIMA

Department of Geology
University of Western Ontario
London, Ontario N6A 5B7, Canada

Abstract

Oriented hematite inclusions in prismatic sillimanite grains from a sapphirine-bearing granulite from Wilson Lake, Labrador, have been studied by optical microscopy and single crystal X-ray precession photography. The inclusions are lath-like in shape, 0.1 to 0.2 μm in smallest dimension, and elongated parallel to the sillimanite **c**-axis. In (001) section they are oriented parallel to sillimanite {110}. The crystallographic orientation of the hematite inclusions is [120] of hematite parallel to **c**-axis of sillimanite, **c**-axis of hematite inclined at 17.7° to the **a**-axis of sillimanite.

Although the hematite–sillimanite phase boundary orientation and hematite lattice rotation are approximately reproduced by two-dimensional lattice misfit (coincident lattice) calculations, significant discrepancies persist between the observed and refined interface parameters. However, further analysis reveals that the observed interface plane is a rational plane in both phases and is parallel to a potential common structural plane. Thus, the orientation of the hematite–sillimanite intergrowth appears to be controlled by topotaxy rather than lattice misfit. Petrographic details suggest that the hematite inclusions formed by a precipitation mechanism (probably exsolution). This is consistent with the complex and extensive retrograde history of the granulites.

Introduction

As discussed in Fleet (1982), minimization of interfacial energy is the dominant factor controlling the shape and orientation of crystalline precipitates and replacement products in minerals. Thus, oriented inclusions tend to have either a topotactic (syntactic) relationship with the matrix phase (e.g., biopyribole intergrowths, Veblen and Buseck, 1980; augite–magnetite symplectites in olivine, Moseley, 1984; magnetite inclusions in orthopyroxene, Fleet et al., 1980) or an orientation which minimizes the dimensional misfit between the strain-free lattices at the phase boundary (e.g., augite–pigeonite intergrowths, Robinson et al., 1977; magnetite inclusions in augite, Fleet et al., 1980; many feldspar intergrowths, Fleet, 1982, 1984, 1985).

Because topotactic interfaces are planes of low lattice misfit and lattice misfit interfaces permit a degree of structural continuity, it is not always possible to clearly distinguish between topotaxy and minimization of lattice misfit. In the present paper, use of these two terms is based on the following criteria. Topotaxy involves a shared structural element and therefore topotactic phase boundaries are usually rational planes. Their orientation is independent of the precise values of the strain-free lattice parameters. On the other hand, phase boundaries defined by minimization of lattice misfit are, in general, irrational, and their orientation is sensitive to change in lattice parameters through change in temperature, pressure, composition, and so on. Thus, if a phase boundary is dependent on the actual values of the lattice parameters, it is regarded as being defined by lattice misfit. If it also coincides with the plane of a prominent structural element it is also topotactic.

In general, lattice misfit boundaries are optimal ones, but when the lattice translation distances along a common third axis are very similar, the misfit is in two-dimensions only and coincidence phase boundaries may be permitted. The orientations of dimensional misfit boundaries are restricted by the following crystallographic law: coincident and optimal phase boundaries have indices (*hkl*) common to both lattices (Fleet, 1982).

Two-dimensional lattice coincident phase boundary theory was developed originally for intergrowths of isomorphous monoclinic phases (e.g., Robinson et al., 1971; Robinson et al., 1977). Fleet et al. (1980) extended its applicability to magnetite–augite intergrowths, which have a monoclinic matrix phase but virtually no topological correspondence between the intergrowth phases. We report here that hematite inclusions in sillimanite, in a sapphirine-bearing granulite from Wilson Lake, Labrador (Grew, 1980), have the superficial appearance of being oriented to lattice coincidence, but, surprisingly, a topotactic explanation appears more appropriate.

Coincident lattice theory for an orthorhombic matrix

Following Fleet (1982), lattices of two different phases are coincident along a common line through (x, 1) when:

$$x = [-B \pm (B^2 - 4AC)^{1/2}]/2A, \qquad (1)$$

0003–004X/85/1112–1232$02.00

where, $A = a_1^2 - a_2^2$, $B = 2(a_1 b_1 \cos \gamma_1 - a_2 b_2 \cos \gamma_2)$, $C = b_1^2 - b_2^2$, and a_1, b_1, γ_1 and a_2, b_2, γ_2 are the two-dimensional lattice parameters. Two non-equivalent orientations of coincidence between the two lattices result when $4AC < B^2$.

For orthogonal lattices (with $\gamma_1 = \gamma_2 = 90°$), equation (1) reduces to:

$$x = \pm(-C/A)^{1/2}, \quad (2)$$

and the two-dimensional lattice theory predicts two symmetry-related lines of coincidence when $-(b_1^2 - b_2^2)/(a_1^2 - a_2^2) > 0$, or $b_1 > b_2$ with $a_2 > a_1$, etc. Thus, for lattice coincidence, inclusions of orthorhombic or higher symmetry within an orthorhombic matrix must be present in two orientations symmetrical to the two-dimensional axes of the matrix phase and parallel to a common third axis (which is normal to the two-dimensional plane). The lattices of the two orientations of the inclusion phase must be rotated symmetrically away from a common reference direction (in the two-dimensional plane) by an amount proportional to the phase boundary orientation. Also, along the common third axis, the translation distance of the two intersecting lattices of the inclusion phase must essentially correspond to the translation distance of the lattice of the matrix phase.

In general, combination of the true space lattices of intergrowth phases may be incompatible with the symmetry requirements of the coincident lattice theory (which, for example, requires a common axis normal to the two-dimensional plane) or may fail to reproduce the observed interface parameters. In such cases one selects a new lattice for the inclusion phase (and, perhaps, also for the matrix phase). Thus, in reproducing the interface parameters for the magnetite-augite intergrowth (Fleet et al., 1980) an equivalent monoclinic unit cell for magnetite was compared with the alternative monoclinic unit cell for augite. In the present study, analysis of the hematite–sillimanite intergrowth starts with the selection of an orthogonal lattice for hematite. Further details are given below.

Petrography and paragenesis

Sillimanite grains with oriented hematite inclusions were obtained from the sapphirine-bearing granulites of the Wilson Lake area, Labrador (62°45W, 53°22N; Department of Mines and Energy, Government of Newfoundland and Labrador sample No. 80VS-132A). The petrology and geochemistry of the metamorphic rocks of this area have been described by Morse and Talley (1971), Leong and Moore (1972), Bourne (1978), Gittins and Currie (1979) and Jackson and Finn (1982). the sapphirine-bearing granulites are heterogeneous coarse-grained rocks with banded texture. Melanocratic bands consisting of sillimanite, sapphirine, orthopyroxene, phlogopite and opaque phases (hematite with ilmenite lamellae and magnetite) are interspersed with leucocratic feldspar-quartz bands. Minor amounts of feldspars and quartz also occur in the melanocratic bands.

Sillimanite occurs as euhedral prismatic grains up to 1 mm in longest dimension, as a fibrolitic overgrowth on prismatic grains, as a narrow rim to sapphirine porphyroblasts and opaque mineral areas, and as euhedral lath-like inclusions within sapphirine. Oriented hematite inclusions are fairly evenly distributed in the medium and sporadic large-sized prismatic grains of sillimanite. However, the grain margins are inclusion-free and adjacent grain boundaries are decorated with small bleb-like grains of hematite. These hematite grains do not contain ilmenite lamellae, which are present in the large hematite grains of the opaque mineral areas. Kink-band boundaries within sillimanite grains are also decorated with hematite inclusions. Small prismatic grains of sillimanite, less than 0.1 mm in diameter, are free of inclusions, as are fibrolitic grains, rims of sillimanite and inclusions of sillimanite within sapphirine porphyroblasts.

Electron microprobe analyses of sillimanite yielded an average formula of $Al_{1.973}Fe^{3+}_{0.035}Si_{0.994}O_5$. TiO_2 and Cr_2O_3 are present in amounts less than 0.01 wt.%. Total iron content varies from 1.58 to 1.80 wt.% Fe_2O_3 and shows no correlation with sillimanite habit. Our data for iron content are comparable to Grew's (1980) results for Wilson Lake sillimanite (1.52 to 2.00 wt.% Fe_2O_3). The maximum iron content reported for natural sillimanite is 2.6 to 2.8 wt.% Fe_2O_3 (Grew, 1980). The calculated formula for our data is close to the formula $(Al_{2-x}Fe^{3+}_x)SiO_5$ proposed by Grew for stoichiometric substitution within the binary system Al_2SiO_5–Fe_2SiO_5. Microprobe analyses of areas of sillimanite grains with hematite inclusions, obtained with a defocussed (10 μm diameter) electron beam, indicated the expected increase in total iron content compared to inclusion-free sillimanite compositions, but TiO_2 was unchanged. Thus, the hematite inclusions appear to be relatively low in TiO_2. The SiO_2 and Al_2O_3 contents of these analyses are comparable to those of inclusion-free sillimanite but, in view of the analytical error ($\pm 0.5\%$), they are not known with sufficient precision to indicate the stoichiometry of homogenized areas of hematite–sillimanite intergrowth.

The opaque mineral areas contain ragged inclusions of sillimanite and sapphirine, and occasional broad tabular lamellae of corundum, which appear consistent with precipitation from a high temperature alumina-bearing oxide phase (e.g., Haslam et al., 1980). The large embayed porphyroblasts of sapphirine contain inclusions of plagioclase and hematite, in addition to sillimanite. Also, the sillimanite rims and fine-grained aggregates of orthopyroxene (with occasional fibrolitic sillimanite) form a complex mantle to sapphirine porphyroblasts and opaque mineral areas, and separate them from quartz and feldspar. As discussed by Morse and Talley (1971), Gittins and Currie (1979), and Jackson and Finn (1982), these textural relations suggest that orthopyroxene and much of the sillimanite were formed by the following retrograde reaction: sapphirine + quartz + hematite → orthopyroxene + sillimanite + O_2.

In summary, the sapphirine-bearing granulites from Wilson Lake are disequilibrium rocks (Grew, 1980). Textural details suggest several retrogressive reactions after

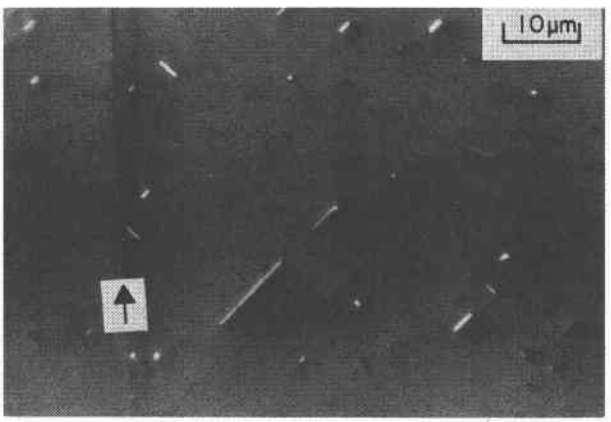

Fig. 1. Optical micrograph of hematite inclusions in a (001) section of sillimanite: arrow indicates (010) cleavage; combined reflected and transmitted, plane polarized light.

peak metamorphism. Exsolution of the oriented hematite inclusions in the prismatic sillimanite grains probably occurred during one (or more) of these retrogressive phases.

Morphology and orientation

The hematite inclusions in prismatic sillimanite grains are lath-like in shape, 10 to 30 μm in longest dimension, and elongated parallel to the sillimanite **c**-axis, as reported by Grew (1980). In (001) section (Fig. 1) they appear to be oriented parallel to sillimanite {110} on superficial examination. Careful measurement in reflected light and on photographic prints yields an inclination toward the sillimanite **a**-axis of $45.7 \pm 0.1°$. This is in good agreement with the calculated value of 45.72° for the interfacial angle $(010) \wedge (110)$. A few inclusions have dimensions as large as 0.5×10 μm in (001) section, but most appear to have dimensions within the range 0.1×1 μm to 0.2×2 μm. The inclusions are sufficiently thin to be translucent in transverse section, with a characteristic orange-red color. Some hematite inclusions are not particularly elongated in (001) section, while others are rounded, even bleb-like, in appearance.

Single crystal fragments of hematite-bearing sillimanite grains were removed from specially prepared uncovered thin sections and examined by the X-ray precession method. Weak hematite reflections are present in zero level, **c**-axis photographs (Fig. 2). Their relative intensity is consistent with a hematite proportion of $\leq 1\%$, in agreement with optical observation. The hematite reflections belong to two symmetry-related *hhl* nets, with the **c***-axis of hematite rotated $17.7 \pm 0.2°$ away from the $-$**a***-axis of sillimanite. In **a**- and **b**-axis precession photographs, *h*00 hematite reflections coincide with 00*l* sillimanite reflections. Other weak reflections on the precession photographs appear to be from randomly oriented feldspar inclusions, which are present in thin section. Their *d*-spacings are inconsistent with quartz.

In summary, the crystallographic orientation of the hematite inclusions (with all positive hematite indices) is [120] of hematite parallel to the **c**-axis of sillimanite, **c**-axis of hematite inclined at 17.7° to the **a**-axis of sillimanite (**a**-axis of hematite inclined at 17.7° to the **b**-axis of sillimanite).

Interpretation

There is a virtual coincidence of the *h*00 (or 0*k*0) reciprocal lattice row of hematite with the 00*l* lattice row of sillimanite. Using JCPDS data, the related lattice spacings are d_{030} (hematite) = 1.454Å and d_{004} (sillimanite) = 1.443Å. $2d_{030}$ of hematite (2.91Å) corresponds to the nearest O–O distance within the (001) close-packed oxygen layers of the hematite crystal structure, and d_{002} of sillimanite (2.89Å) approximately corresponds to the mean nearest O–O distance parallel to the **c**-axis in the sillimanite structure (the repeat distance of the AlO_6 octahedral chains).

In testing for control of phase boundary orientation through lattice coincidence, we adopted the **c**-axis of sillimanite and [120] of hematite as the common third axis and attempted to reproduce the observed phase boundary orientation and lattice rotation using appropriately selected two-dimensional orthogonal lattice parameters: *a* and *c* (or 2*c*/3) of hematite (or ilmenite) and *a* and *b* of sillimanite at room temperature and high temperature (Table 1). All of the present calculations were made with program DIMFIT, originally used in Fleet et al. (1980). Room-temperature lattice parameters for Fe-bearing sillimanite (Grew, 1980) and hematite (JCPDS #24-72) have been extrapolated to higher temperatures using the available thermal expansion

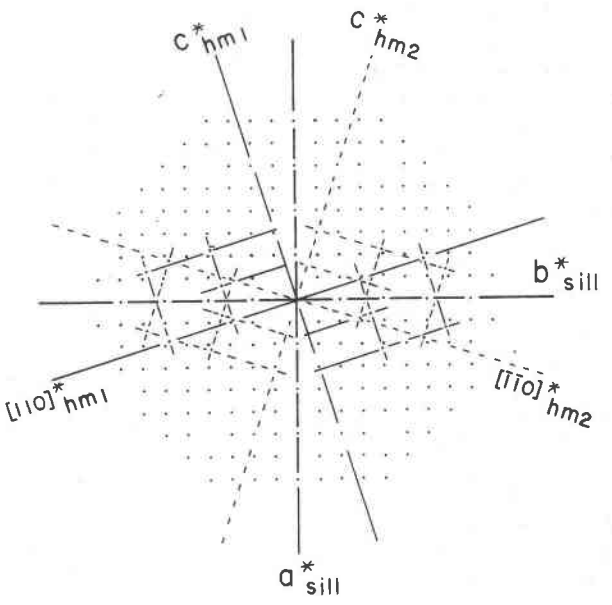

Fig. 2. Interpretation of a precession photograph of a sillimanite grain with hematite inclusions: Mo$K\alpha$; $\bar{\mu} = 25°$; zero level; sill—sillimanite; hm—hematite; precession axis is $\mathbf{c}_{sill}$,$[\bar{1}10]_{hm1,2}$; full lines and broken lines respectively indicate reciprocal lattices of two orientations of hematite inclusions as defined by 110, 220, 113, 116 and 226 reflections.

Table 1. Phase boundary orientation and lattice rotation data for hematite inclusions.

	Orientation Inclination to a_{sill}	Lattice Rotation $c_{hm} \wedge a_{sill}$
hm* in sill, observed	45.7°	17.7°
hm (c'=c)** in sill, RT	63.9	27.8
hm (c'=2c/3) in sill, RT	43.2	16.5
hm (c'=2c/3) in sill, 400°C	43.5	16.6
ilm (c'=2c/3) in sill, RT	45.3	17.2
ilm (c'=2c/3) in sill, 800°C	45.6	17.3

* hm- hematite, sill- Fe-bearing sillimanite, ilm- ilmenite
** All calculations made with a parameter of hematite and ilmenite and a,b parameters of sillimanite

data of Clark (1966, Table 6-1). Lattice parameters for ilmenite are from Wechsler and Prewitt (1984).

The observed phase boundary orientation and lattice rotation clearly are not reproduced with a hematite lattice defined by hematite *a* and *c* parameters (Table 1), but good agreement is obtained with hematite *a* and 2*c*/3. This may be rationalized by appreciating that structural continuity at a coincidence boundary is most logically effected through the ligand (oxygen) substructure. The lattices fitted are essentially those of the oxygen substructures. Thus, the *c*/3 parameter of hematite corresponds to the repeat distance of the oxygen hexagonal close packing along the *c*-axis. The two-dimensional lattice formed by hematite *a* and *c*/3 parameters yields an imaginary solution for the phase boundary orientation (cf. equation (2)). Therefore, the *c*/3 dimension must be doubled. Higher order products of *c*/3 (3*c*/3, 4*c*/3, etc.) also yield real solutions to equation (2) but must result in interfaces with progressively higher interfacial energy due to the increasing proportion of structure out of registry along the interface.

Comparing observed and calculated data (based on a *a*, 2*c*/3 hematite lattice at room temperature), the discrepancies in phase boundary orientation (2.5°) and lattice rotation (1.2°) are comparable with those of unrefined interface parameters in previous lattice coincidence studies on various silicate intergrowths (e.g., Robinson et al., 1977; Fleet et al., 1980) and do not appear too significant in light of the possible variation of lattice parameters with temperature, pressure and composition. However, when the interface parameters are refined by accounting for a moderate ilmenite substitution in hematite and a high temperature of intergrowth formation, apparently significant discrepancies still persist (Table 1). One explanation is that the available lattice parameter data only allow an approximate extrapolation to the parameters at the conditions of intergrowth formation. Another is that the phase boundary may not be defined by minimization of lattice misfit.

In testing for topotaxy, we note that (110) of sillimanite has an inclination toward the sillimanite **a**-axis of 45.7°. Therefore, within the error of measurement, the observed sillimanite–hematite phase boundary coincides with a rational plane of sillimanite. If we fit the (203) plane of hematite to (110) of sillimanite and retain alignment of [120] of hematite and the **c**-axis of sillimanite, the resulting rotation of the hematite lattice is 17.0°, which is similar to the observed lattice rotation of 17.7°. Thus, the observed interface parameters are also consistent with a topotactic control.

In attempting to rationalize this topotactic relationship with the two crystal structures, we find that the oxygen layer parallel to (203) of hematite has nearest-neighbor oxygens in clusters of 4 and 3 (Fig. 3). This oxygen configuration is comparable to that of the (110) oxygen layer in the sillimanite structure, formed by oxgyens close to the plane through the origin. The room-temperature translation distances in this hypothesized common structural plane are 5.82 × 10.47Å for hematite and 5.78 × 10.73Å for sillimanite. In the sillimanite structure, the columns of fourfold clusters of oxygens parallel to the **c**-axis are sections through the AlO_6 octahedral chains. Alternate chains are rotated approximately 90° and are sectioned in the (110)

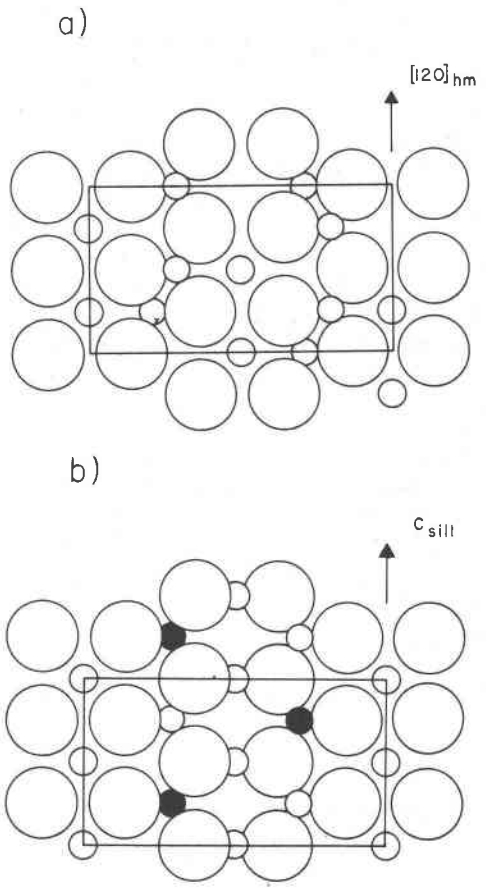

Fig. 3. Schematic representation of: (a) the (203) plane of oxygens in the hematite structure, and (b) the corresponding (110) plane in the sillimanite structure. Rectangle outlines equivalent unit translation distances; cations are placed in ideal structural positions; large open circles, O; small circles, Al and Fe^{3+}; small full circles, Si.

plane to contribute two oxygens per octahedron (dihedral section) in one chain and four oxygens per octahedron (axial section) in the adjacent chain. The threefold clusters of oxygens are faces of the interconnecting (Si, Al)O_4 tetrahedra. In the hematite structure, the four-fold clusters of oxygens in the (203) plane are axial sections through FeO_6 octahedra and unoccupied oxygen octahedra. The threefold clusters are shared faces of oxygen octahedra (both occupied and unoccupied) and tetrahedra (unoccupied).

Discussion

Since the observed interface is a rational plane in both phases and is parallel to a potential common structural plane, and since significant discrepancies persist between the refined and observed interface parameters for lattice coincidence, it seems most probable that the orientation of the hematite–sillimanite intergrowth is controlled by topotaxy. During intergrowth formation, the common structural plane could act as a template for the nucleation of hematite. Structural continuity may be maintained by local coherency stresses at this time.

Why it is not energetically favorable to form a strain-free interface by "fine-tuning" the interface orientation through further lattice rotation is unclear. Obviously, a coincident boundary would result in a decrease in structural continuity. The different degree of correspondence afforded by the potential common structural plane could explain why magnetite forms a coincident boundary in augite (Fleet et al., 1980), while hematite forms a topotactic boundary in sillimanite. The symmetry of the matrix phase may be a factor here also. While lattice misfit is not restricted to monoclinic and triclinic matrix phases, monoclinic and triclinic symmetries do favor interface orientations determined by misfit considerations. Conversely, higher symmetries favor orientations determined by topotaxy.

Either theory adequately accounts for the overall shape of the hematite inclusions, which are elongated in the direction of best dimensional and structural correspondence. Although the precise orientation of the hematite–sillimanite intergrowth does not appear to be controlled by lattice misfit, the coincident lattice calculations were helpful in pointing to the probable interface planes of the topotactic mechanism.

In conclusion, the interface parameters appear to have no bearing on the conditions of formation of the hematite inclusions. However, the petrographic details do suggest that they formed by a precipitation mechanism, and there is abundant evidence that the sapphirine-bearing granulites from Wilson Lake had a complex and extended retrograde history. Quartz from the disproportionation reaction $Fe_2SiO_5 \rightarrow Fe_2O_3 + SiO_2$ was not observed, but the expected small amount, if present as randomly-oriented grains, would be very difficult to detect with any of the techniques used in this study. Also, as discussed by Cameron (1976), the presence of nonstoichiometric sillimanite compositions in higher Fe_2O_3 portions of the Al_2O_3–Fe_2O_3–SiO_2 system cannot be ruled out. Even though the present sillimanite compositions are essentially stoichiometric (cf. Grew, 1980), the preexisting high-temperature Fe^{3+}-excess compositions may have been nonstoichiometric.

Acknowledgments

We thank Andre Thomas (Department of Mines and Energy, Government of Newfoundland and Labrador) for provision of study samples, David Moseley for refereeing the manuscript and D. R. Veblen for editorial assistance. This study was supported by a Natural Sciences and Engineering Research Council of Canada operating grant to M. E. Fleet.

References

Bourne, J. H. (1978) Metamorphism in the eastern and southwestern portions of the Grenville Province. In J. A. Fraser, and W. W. Heywood, Eds., Metamorphism in the Canadian Shield, p. 315–328. Geological Survey of Canada, Paper 78-10.

Cameron, W. E. (1976) A mineral phase intermediate in composition between sillimanite and mullite. American Mineralogist, 61, 1025–1026.

Clark, S. P., Jr. (1966) Handbook of Physical Constants. Geological Society of America Memoir 97.

Fleet, M. E. (1982) Orientation of phase and domain boundaries in crystalline solids. American Mineralogist, 67, 926–936.

Fleet, M. E. (1984) Orientation of feldspar intergrowths: application of lattice misfit theory to cryptoperthites and *e*-plagioclase. Bulletin de Minéralogie, 107, 509–519.

Fleet, M. E. (1985) Orientation of phase and domain boundaries in crystalline solids: Reply. American Mineralogist, 70, 130–133.

Fleet, M. E., Bilcox, G. A. and Barnett, R. L. (1980) Oriented magnetite inclusions in pyroxenes from the Grenville province. Canadian Mineralogist, 18, 89–99.

Gittins, John and Currie, K. L. (1979) Petrologic studies of sapphirine-bearing granulites around Wilson Lake, Labrador. In Current Research, Part A, Geological Survey of Canada, Paper 79-1A, 77–82.

Grew, E. S. (1980) Sillimanite and ilmenite from high-grade metamorphic rocks of Antarctica and other areas. Journal of Petrology, 21, 39–68.

Haslam, H. W., Brewer, M. S., Davis, A. E. and Darbyshire, D. P. F. (1980) Anatexis and high-grade metamorphism in the Champira Dome, Malawi: petrological and Rb-Sr studies. Mineralogical Magazine, 43, 701–714.

Jackson, V. A. and Finn, G. C. (1982) Geology, petrography and petrochemistry of granulite rocks from Wilson Lake, Labrador. Open File Lab. 13E/7(40). Department of Mines and Energy, Government of Newfoundland and Labrador.

Leong, K. M. and Moore, J. M. (1972) Sapphirine-bearing rocks from Wilson Lake, Labrador. Canadian Mineralogist, 11, 777–790.

Morse, S. A. and Talley, J. H. (1971) Sapphirine reactions in deep-seated granulites near Wilson Lake, central Labrador, Canada. Earth and Planetary Science Letters, 10, 325–328.

Moseley, David (1984) Symplectic exsolution in olivine. American Mineralogist, 69, 139–153.

Robinson, Peter, Jaffe, H. W., Ross, Malcolm and Klein, Cornelis (1971) Orientation of exsolution lamellae in clinopyroxenes and clinoamphiboles: consideration of optimal phase boundaries. American Mineralogist, 56, 909–939.

Robinson, Peter, Ross, Malcolm, Nord, G. L., Jr., Smyth, J. R. and

Jaffe, H. W. (1977) Exsolution lamellae in augite and pigeonite: fossil indicators of lattice parameters at high temperature and pressure. American Mineralogist, 62, 857–873.

Veblen, D. R. and Buseck, P. R. (1980) Microstructures and reaction mechanisms in biopyriboles. American Mineralogist, 65, 599–623.

Wechsler, B. A. and Prewitt, C. T. (1984) Crystal structure of ilmenite ($FeTiO_3$) at high temperature and at high pressure. American Mineralogist, 69, 176–185.

Manuscript received, October 31, 1984;
accepted for publication, June 18, 1985.